NASA/TM—2003-212627/REV1

Toward a Fast-Response Active Turbine Tip Clearance Control

Kevin J. Melcher
Glenn Research Center, Cleveland, Ohio

Javier A. Kypuros
University of Texas, Pan American University, Edinburg, Texas

March 2004

The NASA STI Program Office . . . in Profile

Since its founding, NASA has been dedicated to the advancement of aeronautics and space science. The NASA Scientific and Technical Information (STI) Program Office plays a key part in helping NASA maintain this important role.

The NASA STI Program Office is operated by Langley Research Center, the Lead Center for NASA's scientific and technical information. The NASA STI Program Office provides access to the NASA STI Database, the largest collection of aeronautical and space science STI in the world. The Program Office is also NASA's institutional mechanism for disseminating the results of its research and development activities. These results are published by NASA in the NASA STI Report Series, which includes the following report types:

- TECHNICAL PUBLICATION. Reports of completed research or a major significant phase of research that present the results of NASA programs and include extensive data or theoretical analysis. Includes compilations of significant scientific and technical data and information deemed to be of continuing reference value. NASA's counterpart of peer-reviewed formal professional papers but has less stringent limitations on manuscript length and extent of graphic presentations.

- TECHNICAL MEMORANDUM. Scientific and technical findings that are preliminary or of specialized interest, e.g., quick release reports, working papers, and bibliographies that contain minimal annotation. Does not contain extensive analysis.

- CONTRACTOR REPORT. Scientific and technical findings by NASA-sponsored contractors and grantees.

- CONFERENCE PUBLICATION. Collected papers from scientific and technical conferences, symposia, seminars, or other meetings sponsored or cosponsored by NASA.

- SPECIAL PUBLICATION. Scientific, technical, or historical information from NASA programs, projects, and missions, often concerned with subjects having substantial public interest.

- TECHNICAL TRANSLATION. English-language translations of foreign scientific and technical material pertinent to NASA's mission.

Specialized services that complement the STI Program Office's diverse offerings include creating custom thesauri, building customized databases, organizing and publishing research results . . . even providing videos.

For more information about the NASA STI Program Office, see the following:

- Access the NASA STI Program Home Page at ***http://www.sti.nasa.gov***

- E-mail your question via the Internet to help@sti.nasa.gov

- Fax your question to the NASA Access Help Desk at 301–621–0134

- Telephone the NASA Access Help Desk at 301–621–0390

- Write to:
  NASA Access Help Desk
  NASA Center for AeroSpace Information
  7121 Standard Drive
  Hanover, MD 21076

NASA/TM—2003-212627/REV1

Toward a Fast-Response Active Turbine Tip Clearance Control

Kevin J. Melcher
Glenn Research Center, Cleveland, Ohio

Javier A. Kypuros
University of Texas, Pan American University, Edinburg, Texas

Prepared for the
16th International Symposium on Airbreathing Engines
sponsored by the International Society for Airbreathing Engines
Cleveland, Ohio, August 31–September 5, 2003

National Aeronautics and
Space Administration

Glenn Research Center

March 2004

Acknowledgments

This work has been supported by the NASA Power and Propulsion Program through the Revolutionary Aeropropulsion Concepts Project. The authors also wish to acknowledge Bruce Steinetz (NASA Glenn) and Scott Lattime (Ohio Aerospace Institute) for their contributions to ongoing active clearance control research at NASA Glenn Research Center.

Document Change History

This printing, numbered as NASA/TM—2003-212627/REV1, March 2004, replaces the previous version, NASA/TM—2003-212627, December 2003.

The following corrections have been made:

Page 7, section entitled "4.3 Rotor Model," paragraph 1, line 12: The sentence that reads "Error! Reference source not found." has been replaced with "Figure 5."

Text has been added immediately following equation 11 to read: Here, $\delta(t)$ is the overall tip clearance as a function of time. Variables r_{shroud}, r_{rotor}, and l_{blade} are, respectively, the shroud inner radius, rotor tip radius, and blade length as a function of time. Note that, r_a, r_0, and l_0 are the initial geometric state of the shroud, rotor, and blade, respectively; while the subscripted u's denote time-dependent results of previously described deformation calculations.

This report contains preliminary findings, subject to revision as analysis proceeds.

This work was sponsored by the Low Emissions Alternative Power Project of the Vehicle Systems Program at the NASA Glenn Research Center.

Available from

NASA Center for Aerospace Information
7121 Standard Drive
Hanover, MD 21076

National Technical Information Service
5285 Port Royal Road
Springfield, VA 22100

Available electronically at http://gltrs.grc.nasa.gov

TOWARD A FAST-RESPONSE ACTIVE TURBINE TIP CLEARANCE CONTROL

Kevin J. Melcher
National Aeronautics and Space Administration
Glenn Research Center
Cleveland, Ohio 44135

Javier Kypuros
University of Texas-Pan American
Edinburg, Texas 78541

ABSTRACT

This paper describes active tip clearance control research being conducted by NASA to improve turbine engine systems. The target application for this effort is commercial aircraft engines. However, technologies developed for clearance control can benefit a broad spectrum of current and future turbomachinery. The first portion of the paper addresses the research from a programmatic viewpoint. Recent studies that provide motivation for the work, identification of key technologies, and NASA's plan for addressing deficiencies in the technologies are discussed. The later portion of the paper drills down into one of the key technologies by presenting equations and results for a preliminary dynamic model of the tip clearance phenomena.

NOMENCLATURE

Symbol	Units	Description
A	m^2	area
E	Pa	Young's modulus
P	Pa	pressure
T	°C	temperature
c	J/kg-°C	specific heat
h	W/m^2-°C	convection coefficient
k	W/m-°C	thermal conductivity
l	m	blade length
q	W	heat transfer rate
r	m	radius
t	sec	time
u	m	deformation
w	m	width
α	1/°C	thermal expansion coefficient
δ	m	tip clearance
ρ	kg/m^3	density
ν		Poisson's ratio
ω	rad/sec	angular speed
η		film cooling effectiveness

1. INTRODUCTION

Active clearance control is an attempt to improve engine efficiency by manipulating both transient and steady state tip clearances during engine operation. In recent studies,[1, 2] active clearance control (ACC) was identified as one of two technologies most likely to increase the on-wing life of commercial aircraft engines. Additional benefits of decreased operating clearances are reductions in emissions and specific fuel consumption (SFC). An industry rule-of-thumb equates a 0.25 mm (0.010 inch) reduction in turbine tip clearance to a reduction in engine exhaust gas temperature (EGT) of up to 10ºC[1] (18 ºF) and an increase in turbine efficiency of up to 1%.[3] The result would be a reduction in SFC by as much as 1% with a proportional reduction in emissions.[1] Although these benefits appear to be small, a 1% reduction in SFC across the current fleet could save a total of $160M+ per year in fuel costs.[4] It should also produce a significant reduction of total emissions generated by aircraft. These reductions would result in economic and environmental benefits to the public at large.

Lattime[4] describes in detail events that may occur during a flight profile and how they can impact the design of engine clearances. Of particular concern is the pinch point, a minimum clearance condition that can occur during takeoff or reburst. During these events, the rotor assembly expands rapidly, due to centrifugal forces and rapid heating of the turbine blades. At the same time, the surrounding case/shroud structure expands due to thermal effects, but at a much slower rate. The result is a rapid reduction in clearance. In time, the growth rate of the casing exceeds that of the rotor assembly and the clearance increases somewhat. The point in time when the growth rate of the casing first exceeds the growth rate of the rotor is the pinch point. To avoid rubbing at this condition, excess clearance must be designed into the turbine. Unfortunately, this additional clearance results in non-optimal clearances, and increased fuel use at most normal operating conditions, including cruise. In order to realize the full benefit of reduced clearances without damage to the engine, the clearance must be controlled throughout the flight profile.

At present, two approaches are used to minimize operating clearances. The primary approach involves designing clearance variations out of the engine system. This approach relies on material properties and engine operating temperatures to match the growth of turbine subcomponents. In general, this approach allows engine designers to provide optimum clearance at only one operating condition. The second approach also uses a thermal approach to modify the clearance. It involves using fan and compressor bleed air to control the thermal deformation of the case surrounding the turbine. While this approach provides some benefit, it has several limitations. Thermal controls are either model- or schedule-based. Because they use clearance estimates for feedback, or no feedback at all, these controllers cannot currently address clearance changes due to engine wear. Thermal controls are also too slow to mitigate some of the transient events that can occur during a mission. This is due largely to the sizable thermal masses involved. A new approach is clearly needed to realize the full benefit of reduced clearances—a fast-response ACC with direct sensor feedback.

The purpose of this paper is three fold. First, technology development efforts required to realize a fast-response ACC system are identified. Second, NASA's plan for addressing gaps in ACC technology is briefly discussed. Third, one of the technology efforts, a dynamic model of the clearance phenomena, is described in some detail. The discussion is addressed from a control system perspective.

2. CLEARANCE CONTROL TECHNOLOGIES

As a result of recent studies, NASA is pursuing research to improve technologies associated with active control of turbine tip clearance. Efforts are focused on three main areas: control design and system modeling, actuation systems, and clearance sensors. Each of these areas presents unique challenges to the development of a clearance control system.

One challenge for ACC research is the application of control design and dynamic modeling technologies to the problem. Previous NASA efforts in collaboration with industry have quantified tip clearance transients.[5, 6, 7] That significant effort has been expended in this area is obvious from the fact that active thermal-based control systems are flying on commercial aircraft engines. However, current clearance models used by industry tend to be a complex mix of empirical and physics-based equations. They are developed for a specific engine system resulting in proprietary models that are not available in the open literature. Even research that is described in the open literature,[3, 8] uses models based on proprietary data specific to a given, unidentified engine. Because of this, results are difficult or impossible to replicate. A simplified, generic, fist-principles-based clearance model that can be easily adapted to a specific engine is needed for ACC design and evaluation studies.

An important consideration in the design and selection of control laws is the desire to maintain tight operating clearances across the flight trajectory without rubbing. The H_∞-based control synthesis presented by Korson[3] is a useful approach for handling the uncertainties generated by clearance modeling or measurement. It would be instructive to apply this or another robust control synthesis method, first, to higher fidelity models, then, to an actual turbine system.

Another challenge for ACC research is the development of a clearance actuation system that can operate reliably over the flight trajectory and within the severe high pressure turbine environment. Lattime[4] reports that over one hundred patents for passive and active clearance control systems have been filed in the U.S. Passive clearance control systems may be categorized as thermal or pneumatic. Active clearance control systems may be categorized as mechanical, thermal, and pneumatic. The primary clearance control found in large state-of-the-art turbine engines is an active thermal approach that controls clearance by cooling the engine casing with bleed air from the compressor and/or fan. In general, the cooling air is scheduled, though, in more advanced engines, a model-based estimate of the clearance may be used to provide feedback. Those engines that do not employ an active clearance control system generally rely on passive thermal approaches, wherein turbine subcomponents are fabricated from materials with different thermal properties to better match the growth of the rotor assembly with the shroud. In general, thermal systems are too slow to address clearance "pinch points" and other fast transients during the flight profile. Some of the thermal systems also lack sufficient control authority to minimize clearances during cruise where performance benefits are most significant. To be commercially-viable, a new actuation system must overcome the limitations of current systems without significant penalties for cost, weight, or complexity.

A third challenge for ACC research is the development of a turbine tip clearance sensor that is highly-reliable and of flight-quality. Existing turbine tip clearance control systems do not incorporate direct measurement of clearance via sensors. This is due, in part to the inability of existing sensors[9, 10] to meet all of the necessary environmental and operational requirements[4] associated with the turbine. A variety of clearance sensing techniques have been used in a laboratory environment. However, not one of them is currently being used on engines in commercial service.

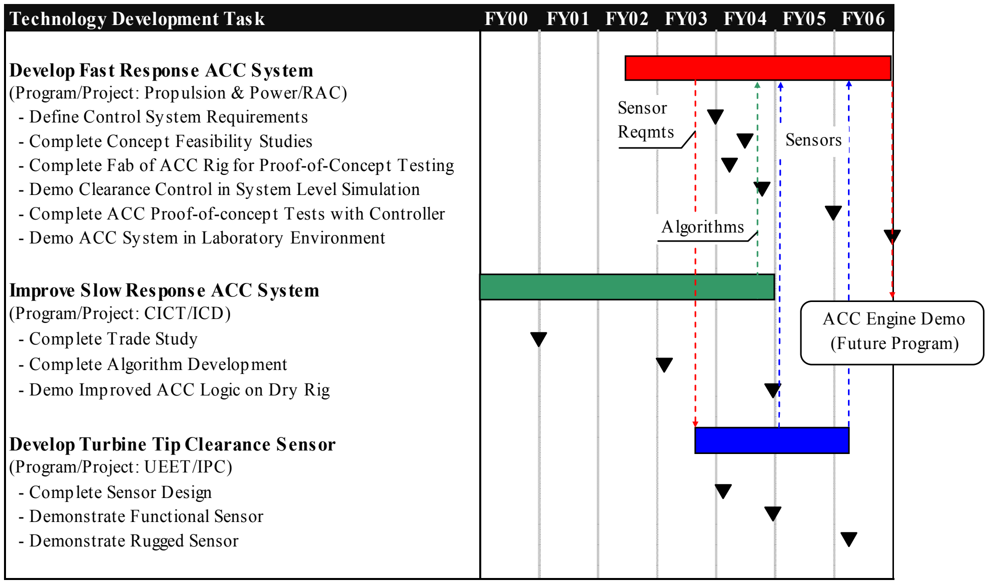

Figure 1. Development of ACC Technologies

3. NASA PLAN FOR CLEARANCE CONTROL RESEARCH

As a result of the significant benefits and high industry interest in active clearance control, researchers and project leaders at NASA Glenn Research Center are working with industry and academia to develop technologies needed to realize such a system. Figure 1 gives a schedule for the current NASA plan.

Technologies needed to support a fast-response ACC are being developed by researchers at NASA Glenn with funding from the Revolutionary Aeropropulsion Components (RAC) Project, part of Power and Propulsion Project at NASA Glenn. Under the effort, researchers are developing prototype actuation systems, dynamic models for predicting clearance, and control laws for a fast-acting turbine tip clearance control. As planned, the initial proof-of-concept demonstration will employ a mechanical system with a state-of-the-art hyrdomechanical positioning system. A successful demonstration could allow a fast-response ACC to replace current thermal-based controls on engine designs that would see service in 10 to 15 years. A second proof-of-concept demonstration that would employ an actuation system based on advanced materials concepts (e.g., shape memory alloys, piezo-electric elements, and magneto-restrictive devices) is envisioned for the end of the project. The target for this technology is future turbine engines that may be driven by fuel cells, electric, or other alternate energy concepts.

Control laws needed to improve current thermal-based ACC systems are being developed by researchers at NASA Glenn in partnership with General Electric Aircraft Engines. The effort is supported by the Intelligent Controls and Diagnostics (ICD) Project, which is part of the Computing, Information, and Communications Technology (CICT) Program. The goal of this ongoing project is to extend the on-wing life of turbine engine systems via modifications to existing control law software. As shown in Figure 1, the effort started with a trade study conducted by General Electric Aircraft Engines. Concluded at the end of FY00, the study identified active clearance control as a key technology for extending engine on-wing life. Additional benefits, previously described, were also found. Control law modifications were completed and implementation initiated by mid-FY03.

The third project involved in developing clearance control technologies is the Intelligent Propulsion Control (IPC) Project which is part of the Ultra Efficient Engine Technology (UEET) Project. The purpose of the UEET-funded effort is to develop and demonstrate a viable tip clearance sensor that can be used in the high pressure turbine. Efforts are currently underway to accomplish this work via contract.

The collaborative natures of the three efforts are denoted by the dashed arrows in Figure 1. Requirements identified by RAC-funded research have been incorporated into a statement of work for the UEET/IPC effort. The UEET/IPC developed sensors will find use in the fast-response ACC control system. Researchers hope that a successful fast-response ACC prototype will merit funding for an engine demonstration from a future project.

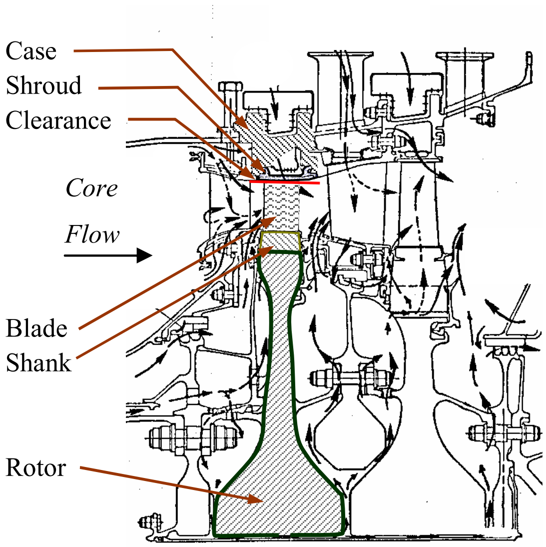

Figure 2. Diagram of high pressure turbine showing elements used in clearance modeling.[5]

4. FIRST-PRINCIPLES DYNAMIC MODEL FOR TURBINE CLEARANCE

The development of control laws for a fast-response ACC requires an experimental or analytical model of the clearance phenomenon. In this section, a first-principles model of the clearance dynamics is presented. The model described in this paper is preliminary, and as such, has limitations. These limitations are being addressed as part of an ongoing effort to improve and validate the clearance model.

In developing a dynamic model of the tip clearance it is instructive to describe the elements of the turbine that effect clearance. Figure 2[5] shows the basic structure of a turbine. The case is the pressure vessel surrounding the turbine. It is designed to be very stiff so that tight tolerances can be maintained during flight. The shroud is composed of a series of circumferential arcs that act as abradable seals limiting the amount of air flow over the blades tips. Each shroud segment is mounted to the case via a rail system that allows for circumferential deformation due to thermal and mechanical loads. Seals between the shroud segments limit leakage flow in the radial direction. The cavity between the case and the shroud acts as a conduit for compressor bleed air used to cool the shroud. Pressure in the cavity is significantly higher than the core air flow pressure to prevent combustion products and unburned fuel from accumulating. The blades are used to convert flow energy to mechanical energy. They are exposed to the largest thermal and mechanical stresses. Blades are mounted to the rotor via the blade shank. In many engines, passages in the blade shank are used to provide compressor bleed air to the blades for film cooling. The rotor, or turbine disk, is the largest rotating element in the turbine. It also rotates at engine speeds and is cooled by compressor bleed air.

For simplicity, the tip clearance model described here incorporates three basic elements – the shroud (or tip seal), the rotor (or disk), and the blades. In order to predict deflections of these elements due to thermal and mechanical stresses, temperature, pressure, and force distributions on each element must be modeled. An engine model, not discussed in this report, is used to generate engine data for a given transient event. The transient data (i.e., speed, temperatures, and pressures) are used by the turbine sub-models to predict deflections due to thermal and mechanical stresses.

Of particular interest here is the clearance. As shown in Figure 2, the clearance is the gap between the blade tip and the shroud. This gap changes during engine operation due to variations in thermal and mechanical stresses associated with each of the turbine elements. The clearance may be calculated by summing the radial position of time-varying geometry of each turbine sub-component as shown in equation (1):

$$\delta(t) = r_{shroud}(t) - \left[r_{rotor}(t) + l_{blade}(t)\right] \tag{1}$$

Here, r_{shroud}, r_{rotor}, and l_{blade} are, respectively, the shroud inner radius, the rotor outer radius, and the blade length – each a function of time.

The bulk of this paper is devoted to describing equations developed to mathematically model the time dependent nature of these geometric parameters. For the sake of brevity, the reader should refer to Kypuros[11]

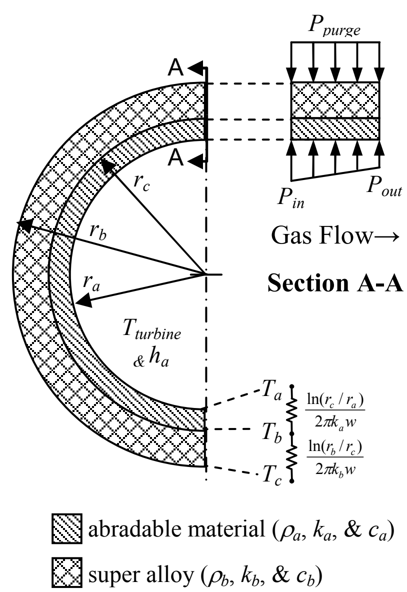

Figure 3. Schematic for Turbine Shroud Model

for derivations. This discussion will start by focusing on the shroud surrounding the turbine.

4.1. Shroud Model

As shown in Figure 3, it is assumed that the general geometry of the shroud is a ring-like structure where the inner surface is coated with an abradable material that also functions as a thermal barrier. The inner surface of the abradable material at radius r_a is exposed to heated gas at a temperature approximately equal to the turbine inlet temperature, $T_{turbine}$. The outer surface of the shroud at radius r_b is exposed to compressor discharge air which is assumed to be at temperature, $T_{compressor}$. Pressure distributions on the inner and outer surface of the shroud are adapted from Lattime.[4] For simplicity, pressure in the tip clearance region is assumed to vary linearly between the turbine inlet and exit pressures. Compressor bleed air is used to purge the space between the shroud and the casing. To facilitate results, it is assumed that the temperature difference between the compressor discharge and the shroud outer surface is negligible.

For the purposes of this study, the abradable material is presumed to function primarily as a thermal barrier and not as a structural member. Due to its conductive properties, the abradable layer dissipates much of the turbine heat, thus reducing the temperature (T_c) otherwise experienced by the superalloy surface at radius r_c. The heat transfer at the inner surface of the abradable material and outer surface of the alloy are assumed to be uniform (quasi-steady) to facilitate a simple model. Heat is convected to the inner surface of the abradable material at wall temperature T_a with a heat transfer coefficient of h_a. The convection coefficient at the outer shroud surface is h_b and the associated surface temperature is T_b.

Before proceeding, the reader should note that equations describing the deformation of the shroud are considered to be the weakest part of this preliminary clearance model. The shroud is actually composed of a series of circumferential arcs attached to the case, rather than the solid structure described here. The case, rather than the shroud, is the supporting structure and should be included in a proper clearance model. Current efforts are focused on revising the model to reflect this fact. Although the solid shroud model does not accurately reflect the engine geometry, the resulting dynamics are similar, and equations presented here will familiarize the reader with the type of analysis required.

4.1.1. Shroud Heat Transfer

To facilitate a closed form solution for the heat transfer between air flowing through the engine and the surface of various turbine subcomponents, heat transfer near the air/material interface is assumed to be governed by the semi-infinite form of the transient heat conduction equation. The classical solution[12, 13] for the surface temperature, T_w, is

$$T_w = \left\{ 1 - \exp\left[\frac{h^2}{\rho c k} t \right] \operatorname{erfc} \sqrt{\frac{h^2}{\rho c k} t} \right\} \left(T_r - T_i \right) + T_i \qquad (2)$$

In this equation, T_i is the initial wall temperature, and T_r is a reference temperature, for this application, the temperature of the conducting air flow.

Kypuros[11] applies this equation to the shroud, and then uses a semi-infinite formulation of the transient heat conduction equation to arrive at an equation for the radial temperature distribution.

$$T(r) = \frac{\ln(r / r_c)}{\ln(r_b / r_c)} \left(T_b - T_c \right) + T_c \, . \qquad (3)$$

Here, subscripts b and c denote the outer shroud surface and the metal/abradable material interface, respectively.

4.1.2. Shroud Deflection due to Thermal Stresses

To enable prediction of shroud deflection due to thermal stresses, it is assumed that the stresses and displacement do not vary over the width of the shroud. The formulation presented herein is equivalent to that given by Timshenko[14] for a thin circular disk with a hollow center. Using Equation (3), Kypuros[11] solves the general equation to obtain a specific solution for the radial deflection due to thermal stresses.

$$u_{s1} = \alpha\, r_c \left[\left(\frac{r_b^{\,2}}{r_b^{\,2} - r_c^2} - \frac{1}{2 \ln(r_b / r_c)} \right) (T_b - T_c) + T_c \right] \qquad (4)$$

Here, T_b is the temperature of the cooling air in the purge cavity, and T_a is the temperature of the air entering the turbine stage.

4.1.3. Shroud Deflection due to Pressure Differential

Timoshenko's hollow cylinder equation is also adapted to predict the deflection of the shroud at the bond radius, r_c, due to pressure differential.

$$\begin{aligned} u_{s2} = {} & \frac{(1-\nu)}{E} \frac{r_c}{r_b^2 - r_c^2} \left(P_o r_b^2 - P_i r_c^2 \right) \\ & - \frac{(1+\nu)}{E} \frac{r_c r_b^2}{r_b^2 - r_c^2} \left(P_o - P_i \right) \end{aligned} \qquad (5)$$

In Equation (5), P_i is the mean internal pressure and P_o is the outer surface pressure. Per Lattime,[4] they are equivalent to $(P_{in} + P_{out})/2$ and P_{purge}, respectively.

4.2. Blade Model

In this section, the term "blade" will be used to describe the "bucket"—the portion of the blade exposed to the primary engine air flow. Of the three basic

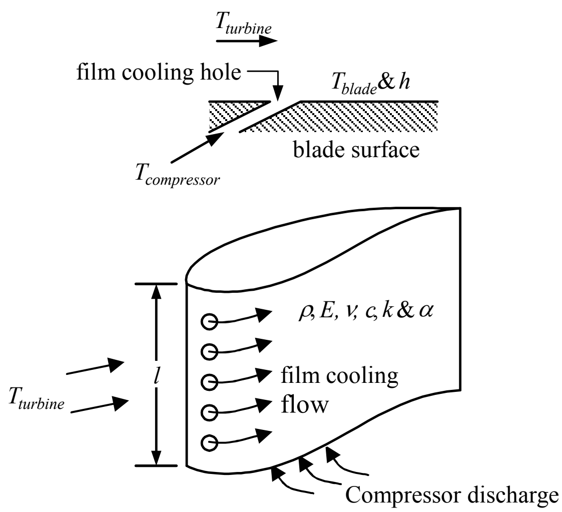

Figure 4. Schematic for Turbine Blade Model

components, this is the most documented. The blade shank could be modeled in a manner similar to that used for the bucket, but with its own thermal and mechanical characteristics. However, due to similarities with the rotor, it will be treated as part of the rotor in this simplified model.

The blades are stressed by both centrifugal forces and thermal expansion. Significant radial deformation of the blades results from centrifugal forces generated by the high rotational speeds. Radial deformation is also caused by large temperature gradients in the engine core flow. Gas temperatures in this region can increase by more than 50% during takeoff and may be on the order of 1300 ºC (2372 ºF) during cruise. To prevent surface temperatures from exceeding the melting point of the blade material, film cooling is employed.

Analysis of the blade deformation is relatively straight forward as heat transfer between the blade and the engine air flow has been studied extensively. Because of this, results for the blade are expected to be more accurate than those for the shroud or the rotor. One aspect of the blade model that should be explored is the inclusion of temperature dependent material properties. Ongoing efforts are addressing this issue and validating the blade model against available data.

4.2.1. Film Cooling of Turbine Blades

In film cooling, a secondary flow is introduced into the boundary layer at the surface of the blade.[15] The temperature of the film cooling fluid, T_f, is much lower than the mainstream temperature, T_m. The blade surface temperature, T_{blade}, may be determined using a semi-infinite formulation similar to equation (2) with the exception that the reference temperature, T_r, is not the mainstream temperature as in two temperature flows. The reference temperature for film cooling is generally unknown and depends on the supply temperatures of the two interacting flows and the degree of mixing that occurs.[12, 13] In such cases, the reference temperature and convection coefficient, h, must be determined experimentally or numerically. Using experimental data, a film cooling effectiveness, similar to that shown in equation (6), is determined in terms of the two flow temperatures, T_m and T_f.[13]

$$\eta = \frac{T_r - T_m}{T_f - T_m}. \tag{6}$$

In the case of the turbine blades, the mainstream fluid, T_m, is at $T_{turbine}$ and the temperature of the film cooling flow, T_f, is assumed to be at $T_{compressor}$. As shown in Figure 4, compressor discharge air enters the blade through the shank and flows into the blade cavity where it exits via film cooling holes at the leading edge. As the flow exits the blade, it creates a thin film of cooler air that wraps around the blade. The temperature of the film-cooled metal is used to compute deformation due to thermal stresses in the blade.

4.2.2. Blade Deflection due to Thermal Stresses

As the temperature of the air surrounding the turbine blade changes, the blade expands or contracts accordingly. Since the blade walls are relatively thin, the thermal gradient of the blade material is assumed negligible. Under this assumption, the blade material will have a uniform temperature equal to the surface temperature, T_{blade}. This approach simplifies the thermal stress analysis to a linear relationship:

$$u_{b1} = \alpha \; l_0 \left(T - T_{ref}\right). \tag{7}$$

Here α is the coefficient of thermal expansion for the blade material; and l_0 is the length of the blade at temperature T_{ref}.

4.2.3. Blade Deflection due to Centrifugal Forces

Radial deflection of the blades is effected not only by changes in temperature, but also by centrifugal forces. The centrifugal forces are proportional to shaft angular speed, $\omega(t)$, the blade mass, m, and the radial distance between the axis of rotation and the blade center of mass, $\sim\frac{1}{2}l(t)+r_o(t)$. Calculation of radial deflection due to the centrifugal forces may be simplified by assuming that the maximum blade and rotor tip growth are sufficiently small so that rotor tip radius and blade length are constant, i.e., $r_o(t)=r_o$ and $l(t)=l_0$. Under this assumption, the time dependency of centrifugal force, F_c, is only a function of shaft angular speed. A simple stress-strain relation adapted from Kypuros[11] can then be used to arrive at the deflection.

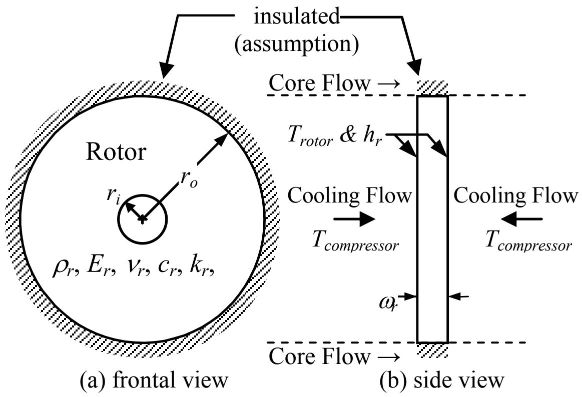

Figure 5. Schematic for Turbine Rotor Model

$$u_{b2} = \frac{m}{\bar{A}_{wall}} \frac{l\left(\frac{1}{2}l + r_o\right)\omega^2}{E} = C_{bl}\frac{\omega^2}{E}. \tag{8}$$

Here, ω may be a function of time, and the value of E may vary with blade metal temperature. To obtain the stress, the force is averaged over the length of the blade using the blade mass, m, and the mean blade wall cross-sectional area, $\bar{A}_{wall}$. In a more general form, C_{bl} is a constant that can be obtained analytically or experimentally for a specific blade geometry.

4.3. Rotor Model

For this study, the rotor model is composed of both the rotor disk and the blade shank. The two are modeled as a rotating disk of uniform thickness, and only deflections due to changes in centrifugal force and purge air temperature are considered. Compressor discharge air is generally used to purge and cool the cavity around the rotor. Only the upper portion of the blade shank is exposed to the high temperature core flow. Thermal expansion is assumed to be dominated by heat transfer between the rotor disk and the compressor discharge air, at temperature $T_{compressor}$. Thus, as shown in Figure 5, the rotor is assumed to be insulated to heat transfer from the turbine blades simplifying the analysis. Compressor discharge air flows over the majority of the rotor's surface area.

Modeling of the rotor is complicated by several factors: a non-trivial geometry, different temperatures on the fore and aft surfaces, and radial temperature distributions due to windage heating. Ongoing modeling efforts are working to ascertain the impact of these effects on the dynamics of rotor deformation.

4.3.1. Rotor Deflection due to Thermal Stresses

As with the outer shroud surface temperature, the rotor surface temperature is assumed to be governed by a semi-infinite formulation similar to equation (2). For the rotor, the reference temperature is the compressor discharge temperature. To facilitate the development of a simplified model, the temperature through the thickness of the rotor is assumed to be relatively constant and approximately equal to the surface temperature (i.e., T_{rotor}=$T_{compressor}$). This assumption does not account for the thermal mass of the rotor. In addition, phenomena that generate radial temperature gradients in the rotor, such as windage heating, are ignored in this model. The current intent is to add effects of these phenomena to future versions of the model as required to improve accuracy.

Since the rotor temperature is assumed to be relatively constant throughout, the thermal strain analysis is significantly simplified and the approximate rotor deflection due to thermal stresses is

$$u_{r1} = \alpha_r r_0 \left(T - T_{ref}\right) \tag{9}$$

where α_r is the coefficient of thermal expansion for the rotor material; and r_0 is the radius of the rotor at temperature T_{ref}.

4.3.2. Rotor Deflection due to Centrifugal Forces

To estimate the rotor tip radial deflection due to centrifugal forces, a simplified equation is used:[14]

$$\begin{aligned} u_{r2} &= \frac{\rho_r \omega^2 r_o}{4E}\left[\left(1-\nu_r\right)r_o^2 + \left(3+\nu_r\right)r_i^2\right] \\ &= C_r \frac{\omega^2}{E} \end{aligned} \tag{10}$$

The first form of the equation shown here describes the radial deflection of a rotating flat disk with a hole in the center where, r_o and r_i are the tip and hub radius respectively. As with equation (8), a more general form is also presented, where constant, C_r, is experimentally or analytically determined from rotor geometry and material properties.

4.4. Clearance Calculation

Expressions for the time varying deflections of the various turbine sub-models due to thermal and mechanical forces can now be summed to obtain the resulting tip clearance. Equation (11) shows how the relative change in the time-varying geometry of each sub-model is used to calculate the overall change in tip clearance.

$$\begin{aligned} \delta(t) &= r_{shroud}(t) - \left[r_{rotor}(t) + l_{blade}(t)\right] \\ &= (r_a + u_{s1} + u_{s2}) \\ &\quad - \left[(r_o + u_{r1} + u_{r2}) + (l_0 + u_{b1} + u_{b2})\right] \end{aligned} \tag{11}$$

Here, $\delta(t)$ is the overall tip clearance as a function of time. Variables r_{shroud}, r_{rotor}, and l_{blade} are, respectively, the shroud inner radius, rotor tip radius, and blade length as a function of time. Note that, r_a, r_0, and l_0 are the initial geometric state of the shroud, rotor, and blade, respectively; while the subscripted u's denote time-dependent results of previously described deformation calculations.

5. MODEL IMPLEMENTATION AND RESULTS

The clearance model described in this report was implemented in the Matlab/Simulink environment. As stated earlier, a dynamic engine model was used to generate the time-dependent inputs for the clearance model. It is important to note that a transient simulation of a large commercial engine was not available during development of this preliminary model. Instead, a simulation representative of engines used on modern fighter aircraft was used to generate the engine transients. The engine transients were then scaled in amplitude and time to approximate the dynamics of a large commercial engine, and they were used as inputs to the clearance model.

A consistent set of data containing all of the necessary model parameters (e.g., geometry, material properties, heat transfer coefficients) was unavailable. Therefore, it was necessary to use estimates for many of the parameters. Kypruos[11] gives a detailed discussion of the sources, confidence level, and associated assumptions used in determining values for the various parameters used in this clearance model.

Results shown in figures 6 and 7 are for a step change in operating condition from ground-idle to maximum power. The time history of the engine speed is shown on the upper axes of Figure 6. Associated temperatures transients for the high pressure turbine and the high pressure compressor are shown on the upper axes of Figure 7. These parameters serve as inputs to the shroud, rotor, and blade sub-models.

In addition to the transient temperature inputs, Figure 7 shows the shroud temperatures and the basic element temperatures. Note that the shroud temperature, T_{shroud}, plotted on the lower axis, is just the average of the bond and outer wall temperatures, T_c and T_b, respectively. As evidenced by the figure, the dynamic temperatures generally follow the expected trend—a relatively slow response compared to the input temperature transients. Data on the lower axes also show that the blade wall temperature, T_{blade}, stays well below the melting point of Inconel 718, which is about 2450 ºF.

Figure 6 shows the individual deflections and overall clearance with reference to the engine speed transient. As expected the rotor initially responds more quickly due to the centrifugal forces induced by the engine speed transient. The shroud catches up and grows more rapidly due to thermal stresses than either the rotor or blades. According to this formulation, the blades contribute the least to the clearance change. Like the rotor, they grow initially quickly due to the rapid increase in centrifugal and thermal stresses, but their growth is significantly less than the rotor. This should be expected considering the relatively short length of the blades compared to the rotor radius. The predicted clearance generally follows the expected trend for a take-off-transient. Engine experience[6, 7] indicates an initial reduction in clearance of about 0.76 to 1.27 mm (30 to 50 mils) and the recovery due to the thermal growth of the shroud is expected to be 0.25 to 0.51 mm (10 to 20 mils). This model predicts a reduction of approximately 0.51 mm (20 mils) and a recovery of about 0.13 mm (5 mils). Exact ranges for a given engine would depend on the parameters and transient conditions specific to that engine. Nonetheless, the results are promising.

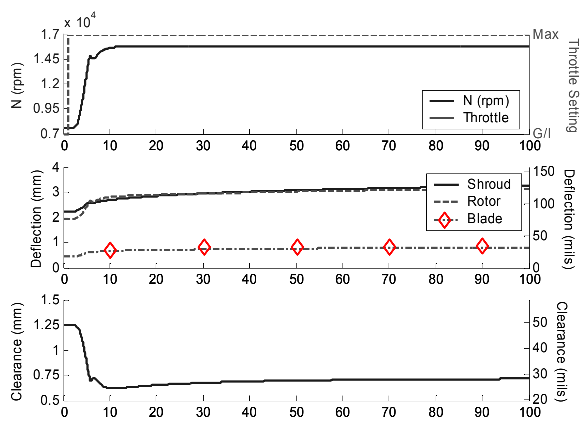

Figure 6. Deflections and clearance for transient from ground idle (G/I) to maximum power

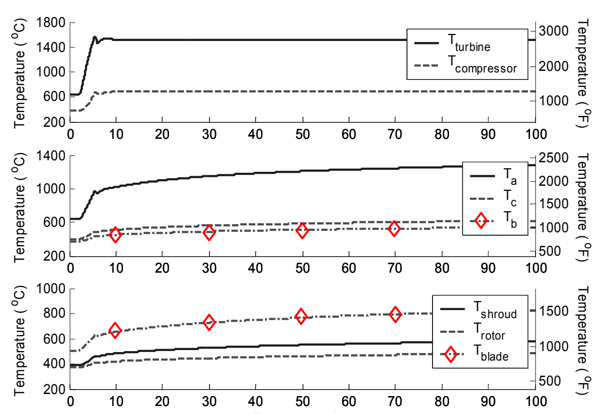

Figure 7. Temperatures for transient from ground idle (G/I) to maximum power

6. SUMMARY

Fast-response active clearance control is discussed as a means of realizing significant benefits for turbine engines in the areas of emissions, fuel savings, and on-wing life. Research in controls & modeling technology, actuators, and sensors are needed to realize these benefits. NASA's plan to develop and demonstrate a proof-of-concept ACC system is presented and the status of current efforts briefly discussed. This is followed by the presentation of a preliminary dynamic model of the clearance phenomenon. Equations describing the thermal and mechanical deformation of turbine subcomponents – the shroud, the rotor, and the blade – are given. Assumptions used in selecting and identifying model parameters are discussed along with limitations of the model. The paper concludes by presenting preliminary results which, though promising, require further investigation and validation.

7. REFERENCES

1. Wiseman, M.W. and Guo, T., "An Investigation of Life Extending Control Techniques for Gas Turbine Engines," Proceedings of the American Control Conference, Arlington, VA, June 25–27, 2001.
2. Final Report: UEET Intelligent Propulsion Technologies, NASA Contract NAS3–9804, Task Order Number 14.
3. Korson, S. and Helmicki, A., "An H_∞ Based Controller for a Gas Turbine Clearance Control System," Proceedings of the 4th IEEE Conference on Control Applications, September 28–29, 1995.
4. Lattime, S. and Steinetz, B., "Turbine Engine Clearance Control Systems: Current Practices and Future Directions," AIAA–2002–3790, NASA/TM—2002-211794, 38th Joint Propulsion Conference and Exhibit, July 7–10, 2002.
5. Halila, E., Lenahan, D., and Thomas, T., "Energy Efficient, High Pressure Turbine Test Hardware Detailed Design Report," NASA CR–167955, 1982.
6. Howard, W. and Fasching, W., "CF6 Jet Engine Diagnostics Program: High Pressure Turbine Roundness/Clearance Investigation," NASA CR–165581, 1982.
7. Olsson, W. and Martin, R., "B747/JT9D Flight Loads and Their Effect on Engine Running Clearance and Performance Deterioration," Nacelle Aerodynamic and Inertial Loads (NAIL)/JT9D Jet Engine Diagnostics Programs. NASA CR–165573, 1982.
8. Jaw, L., "Neural Network Modeling of Engine Tip Clearance," AIAA–97–2775, 33rd Joint Propulsion Conference and Exhibit, July 6–9, 1997.
9. Dhadwal, H., Kurkov, A., and Janetzke, D., "Time-of-Flight Tip-Clearance Measurements," AIAA–99–2134, NASA/TM—1999-209183, 35th Joint Propulsion Conference and Exhibit, June 20–24, 1999.
10. Fotow, A., Mercadal, M., and Tappert, P., "Health Monitoring and Prognostics of Blades and Disks with Blade Tip Sensors, Aerospace Conference Proceedings, IEEE, Vol. 6, pp. 433–440, 2000.
11. Kypuros, J.A. and Melcher, K.J., "A Reduced Model for Prediction of Thermal and Rotational Effects on Turbine Tip Clearance," NASA/TM—2003-212226, March 2003.
12. Kim, Y., Downs, J., Soechting, F., Abdel-Messeh, W., Steuber, G., and Tanrikut, S., "A summary of the cooled turbine blade tip heat transfer and film effectiveness investigations performed by Dr. D.E. Metzger," *ASME Journal of Turbomachinery*, Vol. 117, 1995, pp. 1–11.
13. Kim, Y. and Metzger, D., "Heat transfer and effectiveness on film cooled turbine blade tip models," *ASME Journal of Turbomachinery*, Vol. 117, 1995, pp. 12–21.
14. Timoshenko, S. and Goodier, J., *Theory of Elasticity*, McGraw-Hill Book Company, New York, NY, 1970.
15. Goldstein, R., "Film cooling," *Advances in Heat Transfer*, Vol. 7, 1971, pp. 321–379.

REPORT DOCUMENTATION PAGE

Form Approved
OMB No. 0704-0188

1. AGENCY USE ONLY (*Leave blank*)

2. REPORT DATE
March 2004

3. REPORT TYPE AND DATES COVERED
Technical Memorandum

4. TITLE AND SUBTITLE
Toward a Fast-Response Active Turbine Tip Clearance Control

5. FUNDING NUMBERS
WBS–22–708–87–23

6. AUTHOR(S)
Kevin J. Melcher and Javier A. Kypuros

7. PERFORMING ORGANIZATION NAME(S) AND ADDRESS(ES)
National Aeronautics and Space Administration
John H. Glenn Research Center at Lewis Field
Cleveland, Ohio 44135–3191

8. PERFORMING ORGANIZATION REPORT NUMBER
E–14185–1

9. SPONSORING/MONITORING AGENCY NAME(S) AND ADDRESS(ES)
National Aeronautics and Space Administration
Washington, DC 20546–0001

10. SPONSORING/MONITORING AGENCY REPORT NUMBER
NASA TM—2003-212627-REV1

11. SUPPLEMENTARY NOTES
Prepared for the 16th International Symposium on Airbreathing Engines sponsored by the International Society for Airbreathing Engines, Cleveland, Ohio, August 31–September 5, 2003. Kevin J. Melcher, NASA Glenn Research Center; and Javier A. Kypuros, University of Texas, Pan American University, Edinburg, Texas 78541. Responsible person, Kevin J. Melcher, organization code 5530, 216–433–3743.

12a. DISTRIBUTION/AVAILABILITY STATEMENT
Unclassified - Unlimited
Subject Category: 07 Distribution: Nonstandard

Available electronically at http://gltrs.grc.nasa.gov

This publication is available from the NASA Center for AeroSpace Information, 301–621–0390.

12b. DISTRIBUTION CODE

13. ABSTRACT ***(Maximum 200 words)***

This paper describes active tip clearance control research being conducted by NASA to improve turbine engine systems. The target application for this effort is commercial aircraft engines. However, technologies developed for clearance control can benefit a broad spectrum of current and future turbomachinery. The first portion of the paper addresses the research from a programmatic viewpoint. Recent studies that provide motivation for the work, identification of key technologies, and NASA's plan for addressing deficiencies in the technologies are discussed. The later portion of the paper drills down into one of the key technologies by presenting equations and results for a preliminary dynamic model of the tip clearance phenomena.

14. SUBJECT TERMS
Turbines; Clearances

15. NUMBER OF PAGES
15

16. PRICE CODE

17. SECURITY CLASSIFICATION OF REPORT	18. SECURITY CLASSIFICATION OF THIS PAGE	19. SECURITY CLASSIFICATION OF ABSTRACT	20. LIMITATION OF ABSTRACT
Unclassified	Unclassified	Unclassified	

NSN 7540-01-280-5500

Standard Form 298 (Rev. 2-89)
Prescribed by ANSI Std. Z39-18
298-102